

Post-processing Altimeter Data Towards Coastal Applications and Integration into Coastal Models

9

L. Roblou, J. Lamouroux, J. Bouffard, F. Lyard, M. Le Hénaff, A. Lombard, P. Marsaleix, P. De Mey, and F. Birol

Contents

9.1	Introduction.....	219
9.2	Post-processing Altimetry in Coastal Zones: Early Developments.....	220
	9.2.1 Redefining Editing Strategies	221
	9.2.2 Improving De-aliasing Corrections	222
	9.2.3 Improving the Vertical Reference Frame.....	225
9.3	Latest Upgrades of the X-TRACK Processor.....	227
	9.3.1 Orbit and Large-Scale Error Reduction	228
	9.3.2 High Rate Data Stream	229
9.4	Matching Satellite Altimetry with Coastal Circulation Models	230
	9.4.1 Rationale	230
	9.4.2 Consistency Between Altimeter Measurements and Model Estimates	232
	9.4.3 Methodologies and Case Studies	234
9.5	Concluding Remarks and Perspectives.....	241
	References.....	243

L. Roblou (✉), F. Lyard, M. Le Hénaff, P. Marsaleix, P. De Mey and F. Birol
Laboratoire d'Etudes en Géophysique et Océanographie Spatiales (LEGOS), Université de
Toulouse; UPS (OMP-PCA), 14 Avenue Edouard Belin, F-31400, Toulouse, France and
CNRS, LEGOS, F-31400, Toulouse, France
e-mail: laurent.robrou@legos.obs-mip.fr

P. Marsaleix
CNRS, Laboratoire d'Aérodynamique (LA), F-31400 Toulouse, France

J. Lamouroux
NOVELTIS SA, 2 Avenue de l'Europe, F-31520, Ramonville-Saint-Agne, France

J. Bouffard
Institut Mediterrani d'Estudis Avançats, C/Miquel Marqués, 21, 07190 Esporles, Mallorca,
Illes Balears, Spain

A. Lombard
Centre National d'Études Spatiales (CNES), 18 Avenue Edouard Belin, F-31400, Toulouse,
France

Keywords Coastal altimetry • Data correction retrieval • Data editing • Post-processing • Regional de-aliasing • Synergy with coastal models

Abbreviations

ALBICOCCA	ALtimeter-Based Investigations in COrsica, Capraia and Contiguous Areas
ASI	Agenzia Spaziale Italiana
AVISO	Archivage, Validation et Interprétation des données des Satellites Océanographiques
CLS	Collecte Localisation Satellites
CNES	Centre National d'Études Spatiales
COASTALT	ESA development of COASTal ALTimetry
CTOH	Centre de Topographie des Océans et de l'Hydrosphère
DUACS	Data Unification and Altimeter Combination System
ENVISAT	ENVironmental SATellite
ESA	European Space Agency
EU	European Union
FES	Finite Element Solution
GDR	Geophysical data record
GEOSAT	GEodetic & Oceanographic SATellite
GFO	GEOSAT Follow-On
GMES	Global Monitoring for Environment and Security
GOCE	Gravity field and steady-state Ocean Circulation Explorer
GODAE	Global Ocean Data Assimilation Experiment
GOT	Global Ocean Tide
IB	Inverted Barometer
IMBER	Integrated Marine Biogeochemistry and Ecosystem Research
LA	Laboratoire d'Aérodynamique
LEGOS	Laboratoire d'Études en Géophysique et Océanographie Spatiales
LPC	Liguro-Provençal-Catalan
LSE	Large-scale error reduction
MARINA	MARgin INtegrated Approach
MDT	Mean dynamic topography
MERSEA	Marine Environment and Security for the European Area
MFSTEP	Mediterranean Forecasting System Toward Environmental Prediction
Mog2D	Modèle d'Ondes de Gravité 2D
MSS	Mean Sea Surface
NWMED	North-Western MEDiterranean
OGCM	Ocean General Circulation Model
OSTST	Ocean Surface Topography Science Team
PISTACH	Prototype Innovant de Système de Traitement pour l'Altimétrie Côtière et l'Hydrologie
SARAL	Satellite with ARgos and ALtika

SLA	Sea Level Anomaly
SSALTO	Segment Sol multimissions d'ALTimétrie, d'Orbitographie et de localisation précise
SSH	Sea Surface Height
SST	Sea Surface Temperature
SVD	Singular Value Decomposition
SWOT	Surface Water and Ocean Topography
TOPEX	TOPography EXperiment
TOSCA	Terre, Ocean, Surfaces Continentales, Atmosphère
T-UGOm	Toulouse Unstructured Grid Ocean Model
UNESCO	United Nations Educational, Scientific and Cultural Organization

9.1 Introduction

The raw data provided by radar altimeters onboard satellite missions do not come ready for use. They must be processed to remove unwanted instrumental effects. In the case of SSH estimates, additional information about orbits and auxiliary corrections due to atmosphere and ocean effects need to be applied (Fu and Cazenave 2001). Official altimetry products generally contain sensor measurements, orbit estimations and a full set of corrections (AVISO 1996).

In coastal systems, shorter spatial and temporal scales make ocean dynamics particularly complex, and the temporal and spatial sampling of current altimeter missions is not fine enough to capture such variability (Chelton 2001). Moreover, the error budget of SSH inferred from satellite radar altimetry measurements in coastal regions is increased by intrinsic difficulties that can be separated into two categories.

Firstly, close to the coastline, the altimeter footprint is contaminated by land (and also inland water) surface reflections (Mantripp 1996; Andersen and Knudsen 2000). These surfaces thus contribute to the backscattered power received by the altimeter and significantly affect the shape of the waveform and consequently its tracking by onboard algorithms based on the Brown model (Brown 1977). Returned echoes from the radar altimeter are also often noisy in the coastal zone and the assumption of the Brown model, which is based on specular reflection from the open sea surface, is questionable.

Secondly, environmental and geophysical corrections are less reliable in coastal regions than in open oceans. Environmental corrections derived from onboard instruments (altimeter and radiometer) are contaminated by non-ocean surface reflections (e.g., Ruf et al. 1994; Chelton et al. 2001; Fernandes et al. 2003). Sea state bias correction (i.e. the path delay due to sea surface state) as well as tides and the ocean response to atmospheric forcing have been tailored to deep ocean conditions (e.g., Anzenhofer et al. 1999; Chelton et al. 2001; Le Provost 2001; Carrère and Lyard 2003; Labroue et al. 2004). Finally, the standard altimeter data validity checks are not well suited for coastal regions and often reject many of the measurements acquired close to the coasts (Vignudelli et al. 2000).

These issues limit the effective use of altimeter-derived products in coastal areas (Vignudelli et al. 2005). As a consequence, particular care has to be taken to improve past and current altimeter data reprocessing and corrections.

Since the pioneering effort constituted by the ALBICOCCA (ALtimeter-Based Investigations in COrsica, Capraia and Contiguous Areas) project (Lyard et al. 2003; Vignudelli et al. 2005), various groups are currently working to correct the known weaknesses in the overall processing phase that prevent the use of altimetry in coastal and shelf seas. For example, regional modelling is used to de-alias the tidal and the short-term meteorologically induced signal instead of using global models lacking horizontal resolution (e.g., Jan et al. 2004; Pascual et al. 2006; Bouffard et al. 2008a, b). Other groups are working on the removal of land emissivity in the radiometer footprint for wet tropospheric path delay correction (e.g., Coppens et al. 2007; Desportes et al. 2007; Obligis et al., this volume) or using new waveform models for the retracking of coastal waveforms (e.g., Berry et al. 2005; Deng and Featherstone 2006; Quesney et al. 2007; Gommenginger et al., this volume). More details can be found in the various chapters of this volume. Some of these algorithms (e.g., new retracking algorithms, new radiometer wet tropospheric correction, new regional de-aliasing corrections) are currently being implemented by the French space agency (CNES) and the European Space Agency (ESA) for the definition of new coastal products, within the framework of the PISTACH (Lambin et al. 2008), COMAPI (Lyard et al. 2009), and COASTALT (Cipollini et al. 2008a) project.

This paper discusses the ongoing work at CTOH/LEGOS to reprocess the standard altimeter records by applying adapted strategies for all of the corrective terms of the post-processing stage (the benefit of pre-processing strategies are discussed in detail in the chapter by Gommenginger et al., this volume). Sect. 9.3 presents the latest technical upgrades for higher resolution and multi-satellite monitoring of coastal processes. The physically consistent integration of satellite altimetry into models for coastal ocean analysis is discussed in Sect. 9.4. Finally, Sect. 9.5 presents conclusions and perspectives.

9.2

Post-processing Altimetry in Coastal Zones: Early Developments

The innovative data processing presented hereinafter was originally developed within the framework of the ALBICOCCA project in the North-Western Mediterranean (NWMED) Sea and coordinated by Florent Lyard for the CTOH group at LEGOS, Toulouse, France (Lyard et al. 2003). One of the key tasks of this French-Italian project was to design and implement an altimeter data processing tool adapted to coastal ocean applications (e.g., absolute calibration and drift monitoring of the altimeter, estimation of water transport and validation of numerical models). Additional developments led to the X-TRACK altimeter data processor (Roblou et al. 2007). The objective of this processor is to improve both the quantity and quality of altimeter sea surface height measurements in coastal regions, by tackling all components in the altimeter measurement error budget as recommended by earlier studies (Manzella et al. 1997; Anzenhofer et al. 1999; Vignudelli et al. 2000). This means giving priority to redefining the data editing strategy to minimize the loss of data during the correction phase, by using improved local

modelling of tides and short-period ocean response to wind and atmospheric pressure forcing where possible and by using an optimal, high resolution, along-track vertical reference surface.

9.2.1

Redefining Editing Strategies

The ALBICOCCA project revealed a number of important issues about the use of altimetry for coastal applications. One of them was that current products reject a significant amount of data in the coastal zone not only because of radar echo interferences from the surrounding land but also due to suboptimal editing criteria. The standard validity checks for altimeter data editing have been designed for open-ocean regions. However, the relevance of these checks needs to be re-investigated in coastal systems where particular care is required to select altimeter data of sufficient quality and quantity. Typically, the usual data editing is excessively restrictive close to the coastline, in particular because of the poor spatial resolution of the land flag from the radiometer swath, which limits the amount of exploitable altimeter data in an almost 50 km-width coastal strip. The standard editing criteria are basically built on radiometer or altimeter measurements and/or derived parameters, which are often degraded in accuracy as their footprints are contaminated by the presence of land.

To make the most of coastal altimetry however, we need to go beyond the single point data editing approach. Editing criteria based on thresholds and applied to individual ground-point data are not enough: many data are incorrectly flagged as unreliable because of standard, conservative open ocean flags and editing criteria. Inversely, erroneous data could also be qualified as “good.” The methodology applied for the X-TRACK processor therefore adopts a new data-screening strategy and along-track filtering techniques which allow more data to be recovered in the coastal zone (Lyard et al. 2003).

The guiding principle of this methodology is to screen multiple along-track altimeter data together, rather than individual ground-points. The first step is to maintain all data points where possible in the coastal zone. This implies the use of a high-resolution land mask based on up-to-date coastline data bases and that standard open-ocean editing criteria are not applied. After carefully revisiting the source of the flags, more lenient editing criteria and coastally-dedicated statistical thresholds have been defined (see Table 9.1).

Then, in a second step, avoiding any subjective human procedure, for each single environmental and sea state correction (e.g., wet and dry tropospheric path delay, ionospheric path delay, sea state bias), erroneous corrective terms are detected but not rejected.

Table 9.1 X-TRACK redefined thresholds for data editing in the coastal zone

Parameter	Min. threshold	Max. threshold
Backscatter coefficient (Ku band)	1.0 dB	30.0 dB
Backscatter coefficient (C, S band)	7.0 dB	30.0 dB
Wet tropospheric path delay	-0.5 m	0.0 m
Sea state bias	N/A	0.0 m
Ionospheric path delay	N/A	0.0 m

This second along-track screening flags as “non valid” contiguous measurements of 0-value for sea state bias, wet tropospheric and ionospheric path delays corrections. All previous corrections and the range are also flagged as “non valid” if they are more than three along-track standard deviation from the along-track mean computed from each single valid datasets. Finally, once these valid datasets (meaning altimeter measurements plus associated corrections) are selected, the along-track corrective terms are then filtered and interpolated at the time of the valid range measurements using high order polynomial and minimal curvature interpolation (e.g., Bézier surfaces). As a consequence, this procedure allows invalid correction terms to be retrieved everywhere, where the altimetric range is valid.

Fig. 9.1 shows an example of the data recovery along the TOPEX/Poseidon (T/P) pass 137 for cycle 200 (February 22, 1998). The original GDR wet tropospheric correction from the onboard radiometer is affected by several erroneous values (black curve) in the vicinity of land (i.e. approaching the Portuguese coast, coming-off Spain, approaching and leaving Brittany, crossing the English Channel and overflying the Danish peninsula) which were flagged as bad in the X-TRACK editing strategy. The remaining valid wet tropospheric corrective terms provided by the radiometer are indicated (red curve). De-flagging and re-interpolation of the wet tropospheric correction yields a reconstructed level profile (purple curve). In this example, the large oscillations close to the coastlines induced by land effects are smoothed and the smaller ones over the ocean, assumed to be noise effects, are filtered. Moreover, a corrective term is provided if the range measurement is available and valid (e.g., extrapolation approaching/leaving the coasts, or over a Danish lake).

Birol et al. (2010), Durand et al. (2008) and Vignudelli et al. (2005) outlined the benefits of such a strategy to the overall improvement of altimeter product quality. With respect to standard AVISO products, this innovative methodology allows more altimeter data to be acquired in the coastal zone and ensures better quality for the derived products. For instance, Bouffard et al. (see their chapter in this book) improved the consistency of altimeter sea level anomalies (SLA) estimates with tide gauge sea level by 7% over the NWMED. This concept of working along the satellite track is similarly applied by Tournadre (2006) in his rainfall retrieval studies or by Ollivier et al. (2005) in the framework of their pre-processing of the altimeter waveforms.

9.2.2

Improving De-aliasing Corrections

A second obstacle to tackle when studying coastal ocean processes with satellite altimetry is the aliasing of the tides and short-period ocean response to wind and atmospheric pressure forcing in the altimetry time series. The high frequency energetic variability clearly cannot be resolved by the 10-day, 17-day or 35-day repeat periods of the T/P, Jason-1/2, GFO, ERS-1/2 and Envisat orbits. This high frequency variability appears as noise which is then aliased into lower frequencies. This is a major problem when estimating the seasonal or longer time scale of oceanic circulation in altimeter data. The impact of this aliasing phenomenon is worse for coastal regions because the high frequency signal has larger amplitude in shallow waters (Andersen 1999). The classical solution to this issue is to remove this high frequency signal by using realistic ocean models.

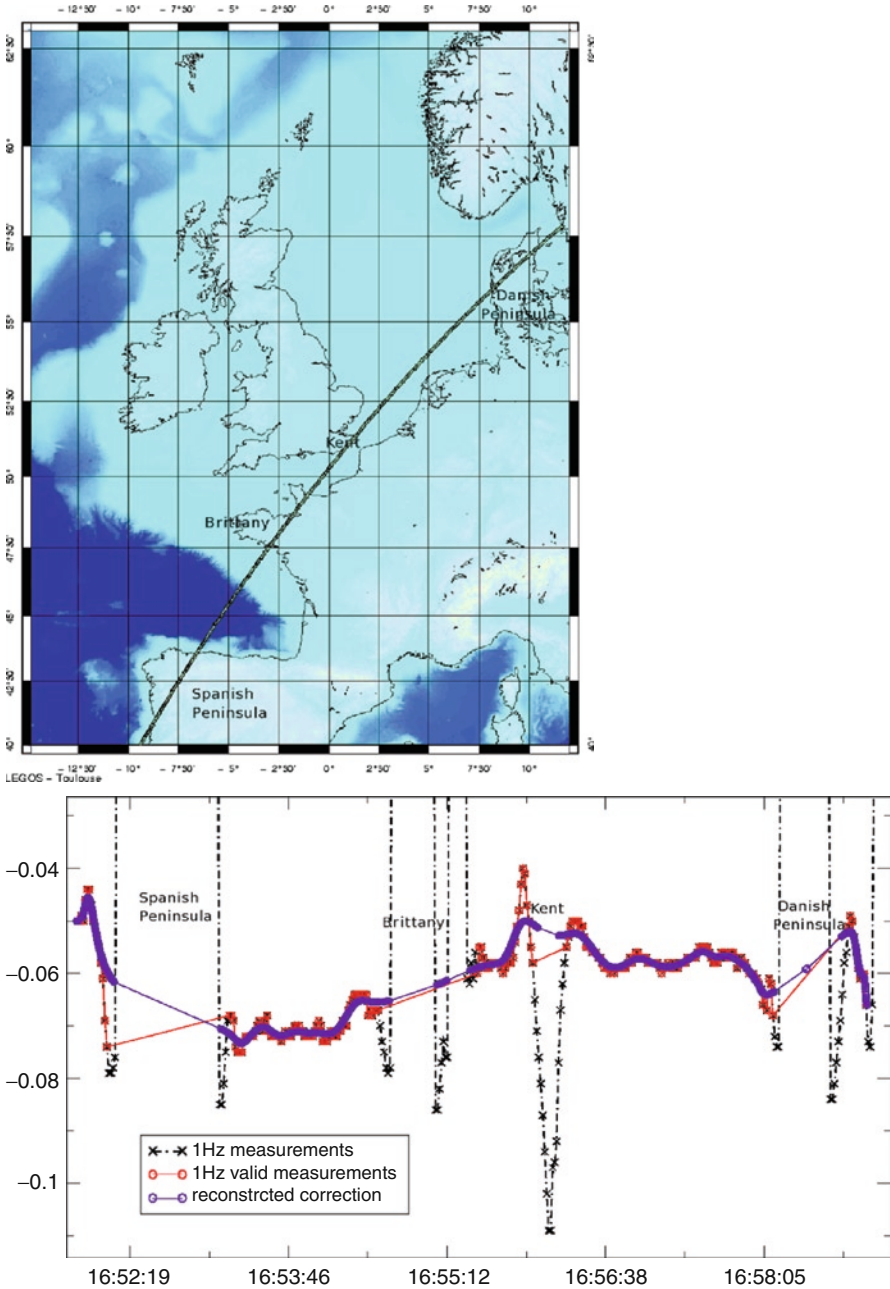


Fig. 9.1 Correction reconstruction. *Left*: geographical location (Western Europe). *Right*: example of wet tropospheric path delay correction (T/P pass 137, cycle 200). Black: raw correction from T/P GDR; red: valid corrective terms as selected by the processing scheme; purple: reconstructed corrective terms for the 10 Hz range measurements. *X*-axis unit is time in hours during February 22, 1998. *Y*-axis unit is meters

However, global ocean models do not provide a precise high frequency, high-resolution correction in terms of both tides and meteorologically forced ocean response in coastal seas and over continental shelves. Indeed, in shallow waters, the propagation of gravity waves is perturbed by numerous factors, e.g., local bathymetry features, the geometry of the shelf and the shorelines, bottom roughness, non-linear interactions, baroclinicity, etc.

Despite their impressive improvement during the past decade and the advent of the precise T/P mission (Le Provost 2001), global tidal models are generally too inaccurate over shallow water areas to fully remove tidal effects from altimeter measurements (see the chapter by Ray et al., this volume). Due to their insufficient spatial resolution, global models cannot resolve rapid changes in tidal features and incorrectly represent the frictional dissipation. Indeed, current global tidal models cannot represent tides in coastal and shelf seas below a decimetre error level. In particular, the omission or the mismodelling of secondary constituents and non-linear tides is largely responsible for the increase in the error budget of global models over continental shelves and along coasts.

In addition to tides, recent results have also shown that atmospherically-forced high frequency signals can be a source of large aliasing in altimeter records at mid and high latitudes (Gaspar and Ponte 1997; Stammer et al. 2000; Hirose et al. 2001; Carrère and Lyard 2003). The atmospheric effects are normally represented by the so-called Inverse Barometer (IB) correction, which is adequate for the open ocean, but known to be unsatisfactory over continental shelves and shallow water seas and at high latitude regions (Carrère and Lyard 2003). In reality, sea surface variation depends both statically and dynamically on meteorological forcing whereas the IB approximation merely formulates the hydrostatic equilibrium between the sea level and the applied atmospheric pressure gradients. Moreover, the IB approximation totally ignores wind-forced sea level variations that can particularly prevail around the 10-day period.

These issues have already been addressed by several teams (Han et al. 2002; Vignudelli et al. 2005; Volkov et al. 2007) and it has been demonstrated that coastal altimetry needs specific, regional models to help reduce the aliasing issue for short-period ocean response to astronomic and atmospheric loading. As recommended by the Ocean Surface Topography Science Team (SALP 2006), the strategy initiated by Lyard et al. at LEGOS is to develop state-of-the-art modelling for ocean response to both astronomic and atmospheric loading. Their approach consists of developing realistic regional models based on the barotropic mode of the T-UGOm code, with additional resolution and locally adapted bathymetry.

The shallow water 2D mode of the T-UGOm code is similar to that previously described in the literature as Mog2D (Carrère and Lyard 2003). Briefly, the code is derived originally from Lynch and Gray (1979) and has since been developed for coastal to global tidal and atmospheric driven applications (Greenberg and Lyard, personal communication). The classical depth-averaged continuity and momentum shallow water equations are solved through a non-linear wave equation with a quasi-elliptic formulation, which improves numerical stability. Currents are derived through the non-conservative momentum equation. A finite element method is applied for converting the problem into a discrete formulation over an unstructured triangular mesh. This spatial discretization method allows a refinement of the model resolution in regions of interest, such as complex coastlines, shallow waters (where most bottom friction dissipation occurs) and areas of strong topographic gradients (showing strong current variability and internal wave generation). It is therefore particularly well

adapted to coastal and shelf modelling of gravity wave propagation. To improve the computational efficiency, a multiple reduced time-stepping scheme is introduced for the purpose of smoothing potential instabilities at model nodes. Carrère and Lyard (2003) and Mangiarotti and Lyard (2008) among others have already shown its efficiency in modelling the high frequency barotropic response to meteorological forcing both at a global and regional scale. The quality of the regional tidal solutions has been highlighted by Pairaud et al. (2008) over the European Shelf or Maraldi et al. (2007) over the Kerguelen Shelf (Southern Indian Ocean) for instance. For these two shelves, the root sum square error of the principal constituents is at least two times lower than for global models.

As a consequence, where possible, local modelling of tides is used preferentially at CTOH/LEGOS in the X-TRACK processor, as an alternative to global open-ocean tide models provided in the standard altimeter products, such as FES2004 (Lyard et al. 2006) or GOT00b (or its updated version GOT4.7). Regional models based on the T-UGOm 2D hydrodynamic code are currently available¹ over the European shelf (Pairaud et al. 2008), over the Kerguelen shelf in the Southern Indian Ocean (Maraldi et al. 2007), over the Caspian Sea (see the chapter by Kouraev et al., this volume) or in the Arabo-Persic Gulf (Lyard and Roblou 2009). In addition, composite spectra can also be designed if the regional tidal atlas exhibits weaknesses. For instance, the K1 constituent solution derived from the regional T-UGOm 2D simulations over the Mediterranean Sea suffers large biases in phase lag over the western basin and leads to greater root mean square differences in comparison to tide gauge observations than for global tidal models (Roblou 2004). As a consequence, it has been replaced by the K1 solution taken from the FES2004 atlas in the optimal spectrum used for the Mediterranean Sea in the X-TRACK processor. Finally, although purely hydrodynamic modelling gives a satisfactory performance compared to the standard global databases (e.g., FES2004, GOT00b or its update GOT4.7), Lyard and Roblou (2009) strongly recommend constraining regional tidal solutions by data assimilation techniques to provide the full required accuracy in the tidal corrections for coastal altimetry.

Regional models of short-period ocean response to wind and atmospheric pressure forcing have been developed or are currently under development based on the same regional meshes as for tides. For example, Cipollini et al. (2008b) used the Mediterranean regional model to correct for high frequency atmospheric variability in a tide gauge data set. They found that the averaged improvement for periods of less than 20 days is 46% in comparison with the IB model and 5% in comparison with the Mog2D-G global model (recommended correction for short-term atmospheric effects). Similar improvements are obtained when de-aliasing an altimeter dataset (see the chapter by Bouffard et al., this volume).

9.2.3

Improving the Vertical Reference Frame

In the absence of a geoid model with sufficient accuracy at small scales which are typical of regional and coastal ocean dynamics, most researchers overcome that difficulty by referencing

¹Tidal atlases are freely available on request on the SIROCCO web site: <http://sirocco.omp.obs-mip.fr/outils/Tugo/Produits/TugoProduits.htm>

the radar altimetry observations to a hydrographic reference surface. The SLA is defined as the difference between the sea levels inferred from satellite altimetry and this reference surface. It is usually approached by the time average of altimeter SSHs, the so-called mean surface height or MSS. However, attention has to be paid to respect the consistency of the corrections applied to the SSH estimates and those applied when building the MSS.

In coastal areas, the resolution of generic MSS products derived from altimetry data is degraded for several reasons. First, altimeter standard data are often missing in the coastal band (from the coastline to 50 km offshore). This implies that the ocean mean sea surface products are merged with a terrestrial geoid model (Hernandez et al. 2000) whose weight becomes predominant in the inverse method applied when building the resulting MSS product. Secondly, the too-sparse altimetry data measurements that are available in coastal and shelf seas are associated with significant errors due to the specific de-aliasing of the short time-space scales of the high-frequency dynamics through the use of global models that are generally too inaccurate in coastal areas. Finally, current satellite gravimeter missions do not provide reliable geoid information for wavelengths lower than 200 km; this results de facto in limited-resolution MSS products.

To overcome some of these problems, the X-TRACK processor allows the possibility of computing a high resolution, along-track mean sea surface consistent with the optimized altimeter dataset and on a high resolution, regular grid following the satellite ground track (Lyard et al. 2003). This along-track MSS is computed on a regular grid ($0.01^\circ \times 0.01^\circ$) following the satellite ground track from an inverse method (optimal interpolation):

$$J(x) = (y - Hx)^T R^{-1} (y - Hx) + (x - x_0)^T B^{-1} (x - x_0) \quad (9.1)$$

where x represents the mean sea surface model vector, y the altimeter data vector and H the observation matrix. The observation matrix uses the coastal-improved altimeter SSHs described in the previous sections. The covariance operator R describes uncertainties on both the instrumental measurements and on the representativeness of the observation operator H . It is assumed to be diagonal (which means that errors are uncorrelated) with observation errors variances set to 20 cm^2 . Covariance operator B describes the Gaussian-shaped uncertainties for the mean sea surface model. Vector x_0 , representing the prior model, is the interpolation of the MSS CLS 01 product onto the optimal model grid. Error variances are set to 0.1 m^2 for the prior model (x_0) and its correlation length is set to the grid resolution, e.g., correlation is 0.5 at 0.01° distance. The resulting MSS thus takes into account the across-track gradient of SSH measurements. The time period over which this average is computed is also an important parameter, as it should take into account typical physical time scales (especially the annual cycle).

Finally, the resulting MSS contains the geoid, the MDT with regard to this geoid and the averaged ocean variability for the period over which the MSS has been computed.

Fig. 9.2 illustrates the mean sea surface obtained following the X-TRACK methodology along the T/P ground track 009. It represents T/P sea level anomalies obtained by computing the mean sea surface using the X-TRACK optimal mean sea surface model (red dots) versus the original GDR correction from the mean sea surface model MSS CLS01 (green dots) for a particular ground track in a near-shore region. Black dots illustrate the mean sea surface difference (i.e. optimal model versus its prior model MSS CLS01) as a function of latitude. The

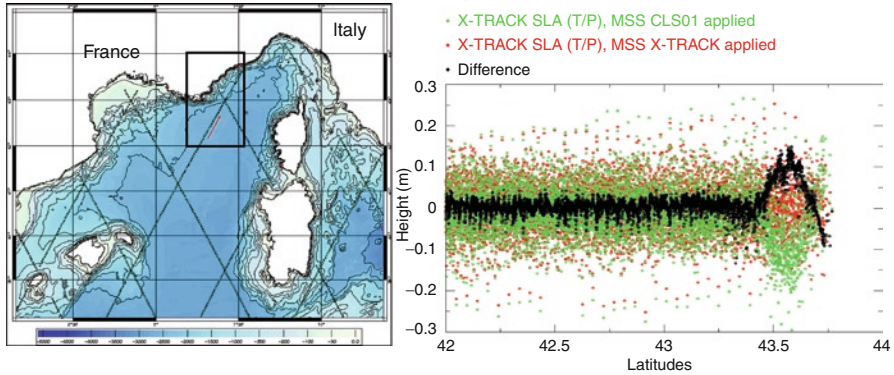


Fig. 9.2 Mean sea surface computed for TOPEX/Poseidon ground track 009 in the NWMED Sea. *Left panel:* location of altimeter passes; *right panel:* T/P SLA including X-TRACK MSS in red dots, including MSS-CLS01 product in green dots and mean sea surfaces differences versus latitude in black dots. (*Y-axis unit in metres*) (Adapted from Lyard et al. 2003)

difference between the X-TRACK optimal MSS and the MSS CLS01 is mainly centred on zero, with oscillations apparently related to MSS CLS01 grid resolution and a bump in the coastal zone. Similar discrepancies have been found for other ground tracks (Lyard et al. 2003). This is a first indication that the X-TRACK optimal mean sea surface model performs better in the near-coast regions, since this higher spatial resolution mean sea surface permits better modelling of the local geodetic variability. These discrepancies could arise from a lack of near-coast altimeter data in the dataset used to derive MSS CLS01, resulting in an imprecise extrapolation between the satellite MSS and the EGM96 geoid in the coastal band.

After such processing, X-TRACK SLAs can be provided² both on their original along-track position (meaning for each individual SSH measurement) and projected onto a mean reference track (meaning that time series are available on a fixed spatial grid).

9.3 Latest Upgrades of the X-TRACK Processor

Based on the X-TRACK along-track altimetry profiles, Durand et al. (2008) have set up a novel methodology for monitoring the East India Coastal current. Their method relies on geophysical parameters such as the length of the first baroclinic Rossby radius of deformation or the maximal acceptable magnitude of the surface current. However, expanding this methodology to other coastal seas like the European seas will need a higher resolution because the first baroclinic Rossby radius of deformation is much smaller there than in the tropics (Chelton et al. 1998). Consequently, observing the complex dynamics of coastal

²Coastal-oriented data sets are computed over several coastal regions and made freely available through the CTOH/LEGOS website: <http://ctoh.legos.obs-mip.fr/products/coastal-products>

Kelvin waves in the mid to high latitudes or western currents along coasts and continental shelves requires ongoing improvement of the space and time sampling of the altimeter products using several satellites (Pascual et al. 2006) and a higher rate for data streams (10 and 20 Hz, e.g., Bouffard et al. 2008a; Le Hénaff et al. 2010).

9.3.1

Orbit and Large-Scale Error Reduction

Taking advantage of multiple satellite missions increases the coverage of the coastal area (Bouffard et al. 2008a), but this does not necessarily improve the quality of the final data product because of the inhomogeneous error budgets between the different satellite altimetry missions. One of the most important sources of error is large-scale orbit error. A Large-Scale Error Reduction (LSER) method designed for regional application has been developed and implemented in the X-TRACK processor. This method, which is not expensive in terms of computational cost, keeps each satellite dataset independent as opposed to a standard dual-satellite crossover minimization (Le Traon and Ogor 1998). Over short distances (arc lengths smaller than 1,500 km), which is the case for most shelf seas, the orbit error can be modelled by a polynomial approximation; it is generally a first order bias and tilt fit (Tai 1989, 1991). The LSER method is based on this previous assumption.

This new algorithm functions as follows. The first step is to compute the time evolution of the along-track-averaged SLA in order to identify large-scale errors. The SLAs used in this algorithm are smoothed along the arc-orbit with a 20 km low-pass Loess filter to reduce the influence of mesoscale dynamics in the calculation of the large-scale error. Only SLAs that are less than two standard deviations from the along-track median value are used. This eliminates spurious data in the coastal zone and allows having consistent geographical coverage when averaging along-track SLAs for each cycle. The black curve on Fig. 9.3 (step 1) shows, such a time series for the GFO track 74 between 2001 and 2005. As shown in Fig. 9.3 (step 1) some large offsets appear in a random way: the averaged along-track SLA suddenly jumps by 10–80 cm within the time span of two cycles. These physically impossible jumps are the consequences of large-scale errors, essentially due to bad orbit determination, and have to be removed. In a second step, the annual and inter-annual signal is removed using a Loess filter in order to eliminate the low frequency signal due to steric effects (see Fig. 9.3, step 2). Then time-averaged statistics (mean and standard deviation) are computed for the spatially-averaged SLA time series. Outliers greater than three standard deviation from the spatial temporal mean of the along-track SLA identify cycles that have to be corrected. The correction consists in removing a bias for the overall ground track of the rejected cycles. The biases are determined with respect to a smoothed version of the along-track averages. The smoothing consists of a combination of Bézier surfaces for smoothing purposes and linear interpolation (see dashed curve in Fig. 9.3, step 3). The previous three steps are integrated into an iterative process in order to select better, discriminate and correct the outliers.

This method is especially well adapted for regional studies. Although it is a very basic orbit and large-scale adjustment, it is sufficient for a regional study, especially when other errors dominate (e.g., data coverage, de-aliasing corrections, land contamination, etc.).

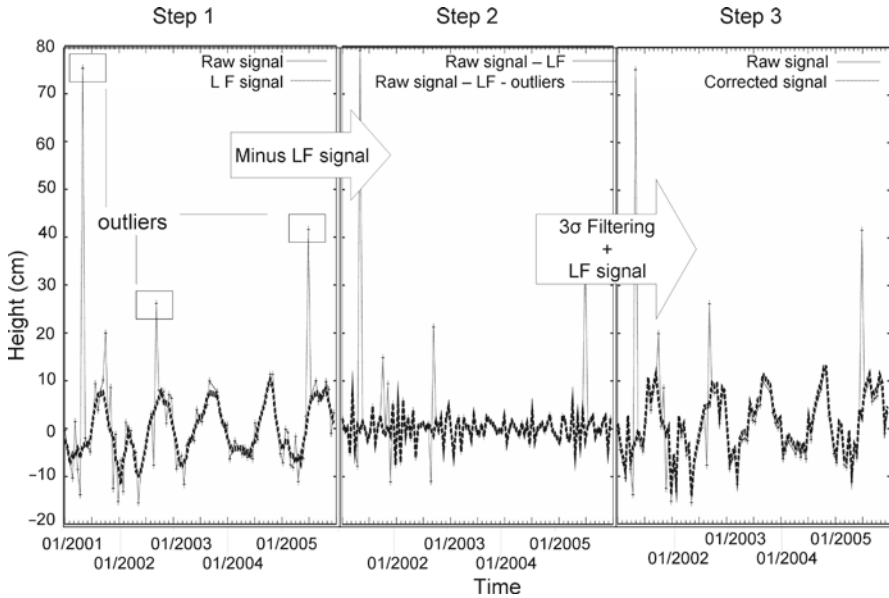


Fig. 9.3 Time evolution of the along-track averaged SLA, GFO track 074. *Step 1*: Raw signal versus low frequency (LF) signal. *Step 2*: Detection and removal of the erroneous cycles by 3σ -filtering of the high frequency signal. *Step 3*: Reconstruction of the corrected signal by a linear regression over a four-cycle time window

9.3.2

High Rate Data Stream

Observing small mesoscale and coastal current sea level variability is a challenging issue which requires intensive spatial sampling. Energetic small-scale ocean dynamics are found along the continental slope and they are very difficult to observe with standard altimetry. The first baroclinic Rossby radius of deformation is generally only a few kilometres and despite a low signal-to-noise ratio, characteristic length scales of energetic disturbances of the coastal currents could be of sufficient size and magnitude to be detected with high-resolution altimetry. The availability of 10/20 Hz values (350–700 m along-track resolution) can provide denser spatial coverage of sea level variability and also enables the estimation of an MSS at a higher resolution along the satellite ground track. The 20 Hz data (respectively the 10 Hz) also allows a closer approach to the shoreline before the single measurement encounters land in its footprint, by reconstructing the 10 (respectively 5) points between the last 1 Hz value available and the coastline (AVISO 1996).

In order to assess the ability of high frequency sampling to observe small coherent dynamic signals rather than noise, Bouffard et al. (2006) computed along-track SLA spatial spectra with all of the T/P ground tracks over the NWMed Sea. For convenience, they performed a time average over all available cycles. The analysis of the spectra shows that the 10 Hz T/P data exhibit the onset of white noise below 3 km, a value much lower than

the standard 1 Hz signal (for which the smallest resolved scale is about 13 km due to the Nyquist-Shannon theorem³). Up to 3 km the signal is dominated by white noise (due to the onboard tracking mode), whereas the oceanographic signal emerges from the noise level at scales greater than 3 km. Similar results have been found for the Jason-1 satellite where the power spectrum shape is slightly different in the small scales due to a different onboard tracking mode but a coherent signal exists for spatial scales greater than 3 km. As a consequence, a 1.5 km high-pass Loess filter is applied to differentiate between high rate orbit and range parameters for the processing of high rate SLAs in the X-TRACK processor.

As demonstrated in Bouffard et al. (2008b) over the Corsica channel area, such a simple post-processing strategy is sufficient to increase the quality and availability of coastal X-TRACK data compared to 1 Hz AVISO standard products. Fig. 9.4 (adapted from Le Hénaff et al. 2010) illustrates the ability of the adopted methodology to retrieve data closer to the coast compared to AVISO regional datasets (e.g., SSALTO/DUACS MERSEA products DT-SLAext), here along the northern coast of Spain. The use of the high rate data stream provides altimeter data with finer spatial resolution and improved temporal sampling. These improvements allow them to study processes associated with the shelf break, such as the slope current, which would not have been possible with classical 1 Hz altimeter products.

However, despite a finer spatial resolution than 1 Hz data, caution is required: this post-processing technique still cannot provide reliable SLAs either at real high frequency sampling (e.g., at length scales of 0.3 or 0.6 km) or right up to the coastline, where the Brown model (used for retrieving ranges to surface from altimeter waveforms) is not automatically well adapted and the altimeter and radiometer footprints are contaminated by land reflections.

9.4 Matching Satellite Altimetry with Coastal Circulation Models

9.4.1 Rationale

There is increasing consensus that coastal management requires a holistic view, based on better quality and more integrated geospatial and environmental information on which a scientifically-sound policy can be built, instead of a sector by sector approach. In the future, an important, international research effort will be made on coastal zones (within the GMES and IMBER initiatives) and will aim at developing operational oceanography and services

³In essence, the Nyquist-Shannon sampling theorem asserts that an analog signal that has been sampled can be reconstructed from the samples if the sampling rate exceeds $2N$ samples per second, where N is the highest frequency in the original signal. In the case of the T/P satellite, 1 Hz sampling along the satellite ground track represents 6–7 km spatial sampling (depending on the latitude of the satellite), meaning that only scales greater than about 13 km can be reconstructed from the samples.

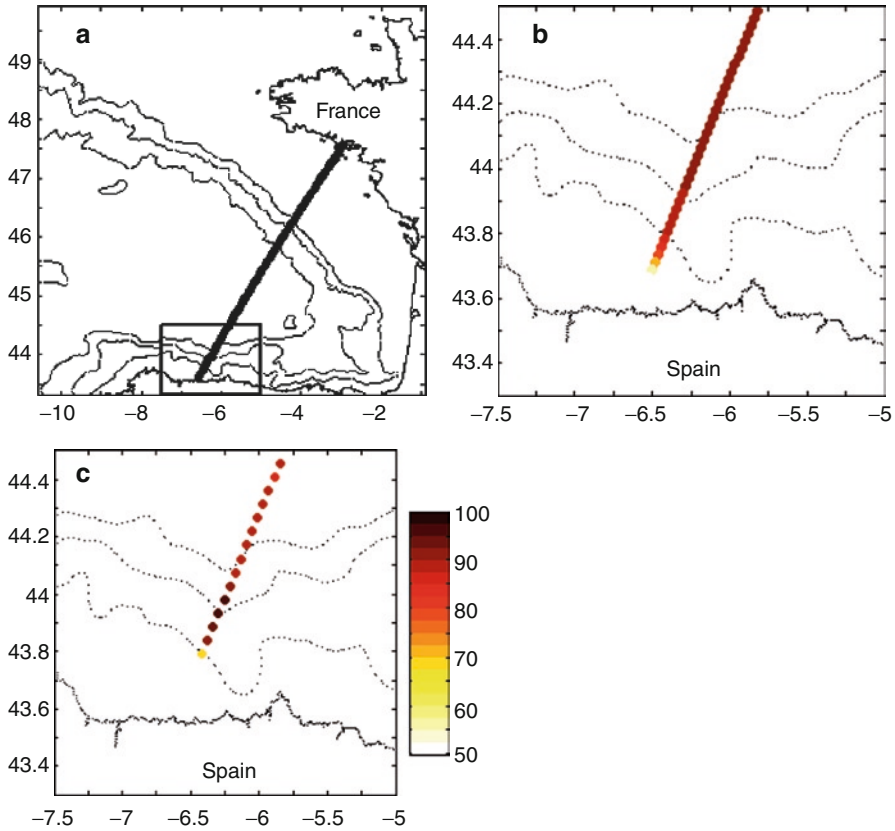


Fig. 9.4 Zone of study (a) and altimeter data coverage close to the northern Spanish coast for TOPEX/Poseidon track 137 (November 1992–August 2002), for (b) X-TRACK dataset – 2 Hz data interpolated from the high rate 10 Hz data stream – and (c) AVISO 1 Hz dataset. In grey scale is the temporal coverage (% of the total number of cycles available). In dotted lines are the 200, 1,500, and 4,000 m bathymetric contours

at regional and coastal scales. As for the deep ocean, regional operational oceanography will be made possible only in an integrated approach, merging process-oriented studies, remote-sensed and *in situ* observation systems, ocean modelling and data assimilation.

Ocean modelling is a precious tool for studying physical processes because all state variables of the system can be accessed. However, models only partially represent the true state of the ocean. Data assimilation of satellite altimetry can thus help in reducing model errors. Data assimilation of coastally-improved satellite altimetry (e.g., CTOH/LEGOS SLA products based on X-TRACK processor, forthcoming COASTALT and PISTACH datasets, etc.) could be highly valuable for regional circulation and even for deep convection studies. At a more local level, a realistic representation of regional circulation is required for the study of the current-shelf/slope interactions or more coastal processes. Although satellite altimetry is not capable of direct monitoring of such small-scale coastal

phenomena as wind-induced processes or upwelling systems, the observations it provides of regional oceanic features will still enhance the realism of coastal models through improved monitoring of the offshore circulation by data assimilation.

The objective of the following section is to address the issue of an optimal matching of improved, coastal-oriented altimeter observations with regional hydrodynamic model sea surface elevation estimates. Methodologies of matching are proposed and the results of case studies are discussed.

9.4.2

Consistency Between Altimeter Measurements and Model Estimates

Once a reference level is removed and the effects of tides and short-period ocean response to wind and atmospheric pressure forcing are corrected, the most important component of satellite-observed sea level variability on a seasonal timescale is due to the so-called steric effect. This can be defined as the variation of the sea level due to the expansion/contraction of the ocean water volume in response to density changes in the whole water column (see Lombard et al. 2006). This steric expansion/contraction is an ocean process of first importance when it comes to local sea level variations in the seasonal and inter-annual time scales (e.g., Pattullo et al. 1955; Church et al. 1991; Gregory 1993), and its surface signature is added to the seasonal and inter-annual surface variations due to ocean dynamics.

9.4.2.1

Steric Effect Surface Signature

From a physics standpoint, the sea level change caused by steric effect, h , can be estimated by integrating the density anomalies over the whole water column (Tomczak and Godfrey 1994):

$$h(\lambda, \varphi, t) = \int_{-H}^0 \frac{\rho(\lambda, \varphi, z, t) - \rho_{\text{ref}}(\lambda, \varphi, z)}{\rho_{\text{ref}}(\lambda, \varphi, z)} dz, \quad (9.2)$$

where the density ρ is a function of the longitude λ , the latitude φ , the depth z and the time t , ρ_{ref} is a characteristic density over the area depending only on the geographical location and depth, and H is the total water depth. Considering the UNESCO state equation that links the sea water density to its temperature and salinity (UNESCO 1981), the sea level change caused by steric effect only depends on temperature and salinity variations in the water column.

Even if the thermal-steric contribution of the ocean upper layers can account for most of the sea level variations, the thermal-steric contribution of the deeper ocean layers, as well as the halo-steric contribution, should not be neglected at the regional scale. In particular, recent works have demonstrated that the halo-steric contribution (coming from salinity freshening due to fresh water input by river discharge, evaporation, precipitation, ice melting, etc.) can locally balance the thermo-steric effects, in particular in the Northern Atlantic ocean (Antonov et al. 2002; Ishii et al. 2006; Wunsch et al. 2007; Köhl and Stammer 2008; Lombard et al. 2009). In the same way, the thermal-steric contribution of

the deeper layers can explain the sea level variations in the Southern Ocean (Morrow et al. 2008; Lombard et al. 2009).

Recent studies (Carton et al. 2005; Lombard et al. 2009) have shown that the regional variations of the steric effect signature mostly result from the general ocean circulation in response to wind and atmospheric pressure forcing (through the buoyancy forcing term). Heat fluxes and fresh water inputs could also account for a significant part, in particular in the Southern Ocean and in the Northern hemisphere (Köhl and Stammer 2008). In addition, these seasonal low frequency phenomena are also enhanced by the sea level trend caused by global warming. It has been shown that its impact on coastal seas and its regional discrepancies can be significant (e.g., Lombard et al. 2009).

9.4.2.2

Steric Height in Coastal Ocean Models

Regional and coastal circulation models mainly feature a solution of the free surface which satisfies the primitive equations. In addition, these models generally formulate the hydrostatic and the Boussinesq hypotheses, respectively assuming negligible vertical velocities and volume conservation (rather than mass-conservation). For the sake of convenience, the model assuming the volume conservation will be referred to in the following lines as the “Boussinesq model.”

Compared with the basic situation described in the left side of Fig. 9.5, a uniform temperature flux entering the upper layer of the left column generates a decrease of the density in this column. The upper layer water column then expands and its thickness increases from h_2 to $h_2 + dh$ (in the middle part of Fig. 9.5). Due to the fact that the total mass of

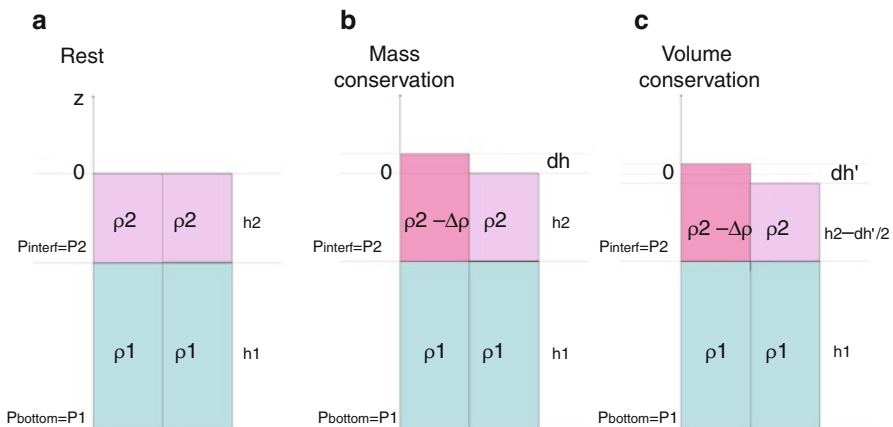


Fig. 9.5 Steric effect modelling in mass-conserving and volume-conserving models – simplified scheme. (a) Representation of two water volumes at rest and subjected to a uniform heat flux coming into the upper layer of the left-hand volume. (b) Free-surface adjustment of a mass-conserving model. (c) Free-surface adjustment of an incompressible volume-conserving model

each column is unchanged, the hydrostatic pressure at the interface also remains unmodified in both columns.

The conservation of mass in the water columns presupposes that:

$$(h_2 + dh) \times (\rho_2 - \Delta\rho) = h_2 \times \rho_2 \quad (9.3)$$

where h_2 is the height of the upper layer of density ρ_2 , dh is the rise of sea level induced by the variation of density $\Delta\rho$ (see left side and centre of Fig. 9.5).

Consequently,

$$dh = h_2 \times \Delta\rho / (\rho_2 - \Delta\rho) \quad (9.4)$$

Assuming, that the variations of density are much smaller than the density itself (generally with a ratio of 1 for 1,000), the sea surface elevation due to the expansion of the left column in Fig. 9.5 can be approximated by:

$$dh = h_2 \times \Delta\rho / \rho_2 \quad (9.5)$$

In the Boussinesq model (see right side of Fig. 9.5), it is assumed that the fluid is incompressible, which implies that the expansion of the total volume (i.e. the volume of both columns) is null. On the other hand, one can assume that, at a regional scale, the dynamic response of the model should imply a modification of the column height in order to keep the hydrostatic pressure at the interface constant, i.e.

$$(h_2 + dh'/2) \times (\rho_2 - \Delta\rho) = (h_2 - dh'/2) \times \rho_2 \quad (9.6)$$

where h_2 is the height of the upper layer of density ρ_2 , dh' is the rise of sea level induced by the variation of density $\Delta\rho$ (see right side of Fig. 9.5).

Finally,

$$dh' = h_2 \times \Delta\rho / (\rho_2 - \Delta\rho / 2) \quad (9.7)$$

In the same way, since the variation of density $\Delta\rho$ is much smaller than the density ρ_2 :

$$dh' = h_2 \times \Delta\rho / \rho_2 \quad (9.8)$$

As a result, the incompressible Boussinesq models are able to reproduce the realistic difference of height between the heated column and the cold one. On the other hand, these models do not reproduce the mean sea surface rise, i.e. they do not reproduce the mean steric effect over the modelling area. In other words, in these models, the spatial variability of the steric effect is taken into account but its mean time variation is zero, due to the Boussinesq approximation. This, for example, removes part of the seasonal steric effect and any mean sea level rise.

9.4.3

Methodologies and Case Studies

Once the correction of tides, short-period wind and atmospheric pressure effects and a reference level has been applied, combining altimetry observations and coastal circulation models can be reconsidered as a combination of altimetric and modelled sea level anomalies.

The sea level anomaly observed in the altimetry measurements is mainly dominated by the surface signature of the seasonal steric effect, which is generally not reproduced by coastal circulation models. To account for this, either the steric effect contribution needs to be removed from altimetry or added to the model. In the following section, we will consider both of these approaches.

However, the following discussion is a first step of an ongoing effort at CTOH/LEGOS to address the issue of matching altimeter-derived estimates and hydrodynamic models in the coastal systems. The methodologies are here assessed in a pilot system, the NWMED Sea. They need to be implemented and tested in other coastal and shelf seas before providing the community with any guideline, and in particular for an operational correction.

9.4.3.1

Modelling Approach

Strategy

Greatbatch (1994) showed that it was possible to correct the modelled free-surface elevation computed with models taking into account the Boussinesq approximation by adjusting a specific constant. This adjustment constant is spatially uniform over the modelling area, but has a time variability taking into account the net expansion/contraction of the ocean. Furthermore, this correction, being spatially uniform, has no dynamic impact on the current velocities computed by models. The methodology proposed here consists of preferentially removing the steric effect contribution from the altimeter measurements.

Based on the sea water state equation, the density field can be obtained from the model salinity and potential temperature fields at the time of the altimeter measurements. Then, in order to avoid local differences, the resulting steric sea level elevation field needs to be smoothed over a large enough area (e.g., by averaging over the whole regional domain). Finally, this mean steric change would preferably be averaged over a window of several days, since only its low frequency time variability is required in the case of regional and coastal models.

In order to exclude all steric change processes with non-zero average contribution over the run period, a second corrective term should be added, taking into account the mean model sea surface elevation and the mean steric height differential over the study period. In practice, the choice of the averaging period is initially made from the start and end dates of the model run, so that in a second step altimeter SLAs are consistently averaged over the same period.

As a consequence, a steric correction from model simulation outputs can result as follows:

$$\delta = \left(\overline{h_{steric}(x, y, t)}^{\text{domain}} \right)_{LF} - \left(\overline{\eta(x, y, t)}^{\text{period}} + \overline{h_{steric}}^{\text{domain, period}} \right) \quad (9.9)$$

where δ is the adjustment constant to apply, h_{steric} is the steric surface signature on the model grid points (x, y) and at time t of observations, η is the model sea surface elevation at grid points (x, y) and at time t of observations; the overbar \overline{X}^P denotes the average of X over period P and $(X)_{LF}$ denotes the low-passed filtering of X .

Model Data

The hydrodynamic model used for this case study is the three-dimensional, primitive equation coastal ocean model SYMPHONIE (Estournel et al. 1997; Marsaleix et al. 2006). It is in widespread use for shelf circulation, sediment transport and coupled bio-physical applications (e.g., Estournel et al. 2003; Dufau-Julliand et al. 2004; Petrenko et al. 2005; Ulses et al. 2005; Gatti et al. 2006; Guizien et al. 2006; Jorda et al. 2007; Hermann et al. 2008). This model is based on the hydrostatic assumption and the Boussinesq approximation. It is eddy-resolving. The three components of the current, the free-surface elevation, the temperature and the salinity are computed on an Arakawa C grid (Arakawa and Suarez 1983), using an energy-conserving finite difference method (Marsaleix et al. 2008). A hybrid sigma-step coordinate system is used for the vertical discretization and a curvilinear coordinate for the horizontal discretization. More details on the model characteristics can be found in Marsaleix et al. (2008). For this study, the model was run over the NWMED Sea from September 2, 2004 to February 28, 2005, on a 3 km horizontal grid spacing which is about three times smaller than the first baroclinic Rossby radius of deformation in this area, of about 10 km. The model is one-way nested on a daily basis into the MFSTEP project OGCM (Estournel et al. 2007). Fig. 9.6 displays the bathymetry of the regional model simulation.

Coastal Altimeter Data

SLA estimates were computed with the X-TRACK processor for the four altimetry missions available over the study period, namely TOPEX/Poseidon, Jason-1, Envisat

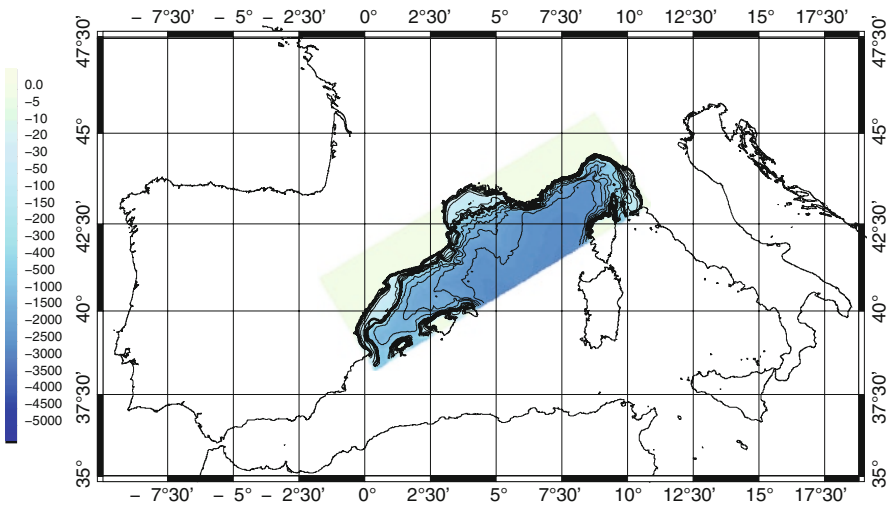


Fig. 9.6 SYMPHONIE model bathymetry for the NWMED Sea configuration

and GFO. The altimeter data were corrected for environmental and sea state perturbations, applying the edition/rebuilding procedure as described in previous sections; the tidal correction was computed from a composite spectrum based on the T-UGOm 2D for all constituents except K1 which was taken from FES2004; atmospheric loading effects have been corrected based on the T-UGOm 2D regional model simulations and the MSS was computed over the model run period (02/09/2004–28/02/2005) as recommended previously. The steric effect surface signature was corrected using the model itself, applying Eq. 9.9 1 Hz SLA estimates were provided along the ground track.

Results and Analysis

Model elevations are first compared with altimeter estimates. Fig. 9.7 displays examples of comparisons between the SLA derived from both model and altimeter along different satellite tracks. These comparisons between model outputs and observations globally show good agreement in the typical synoptic scale and mesoscale. The slopes and large-scale structures represented in the model simulation are close to those captured in the altimeter observations (a low-pass filter would highlight this feature). Moreover, altimeter data seems to provide additional information at scales shorter than 50–60 km that are not represented in the model simulation.

In addition, Fig. 9.8 represents the spatial power spectra of model elevation (blue curve) and corrected SLAs from the T/P altimeter (red line). It can be noticed that short scales (less than 10 km) are not present in the model, which is not surprising owing to the 3 km resolution of its horizontal grid. For wavelengths between 10 and 60 km, the model and altimeter data represent the same level of energy, implying an overall, statistical agreement for these scales.

In this example (Fig. 9.7b), an offset of nearly 10 cm can be seen between the model elevation and the altimeter measurement (along GFO track 401). This bias is also observed for a coincident Jason-1 pass. As the two satellites are independent, it cannot be residual orbit error but is more probably due to an internal error in the computation of the steric correction at that time. The time variation of the sea surface elevation spatial average in a Boussinesq incompressible model depends on the net flux of water at its lateral boundaries. In the present case, it thus depends on the sea surface elevation provided by the OGCM. If the sea surface elevation is erroneous in the OGCM, it introduces an error on the coastal model sea surface elevation through the open boundary forcing and then in the computation of the steric correction. Hopefully, this kind of error does not affect regional circulation modelling, which primarily depends on the sea surface elevation gradients rather than on the absolute value of the sea surface elevation. However, when assimilated, such an outlier will inevitably have an impact on the analysis solution and smart techniques have to be implemented in the assimilation schemes to prevent this spurious model adjustment (e.g., by placing an upper limit on the difference between model proxy and observation).

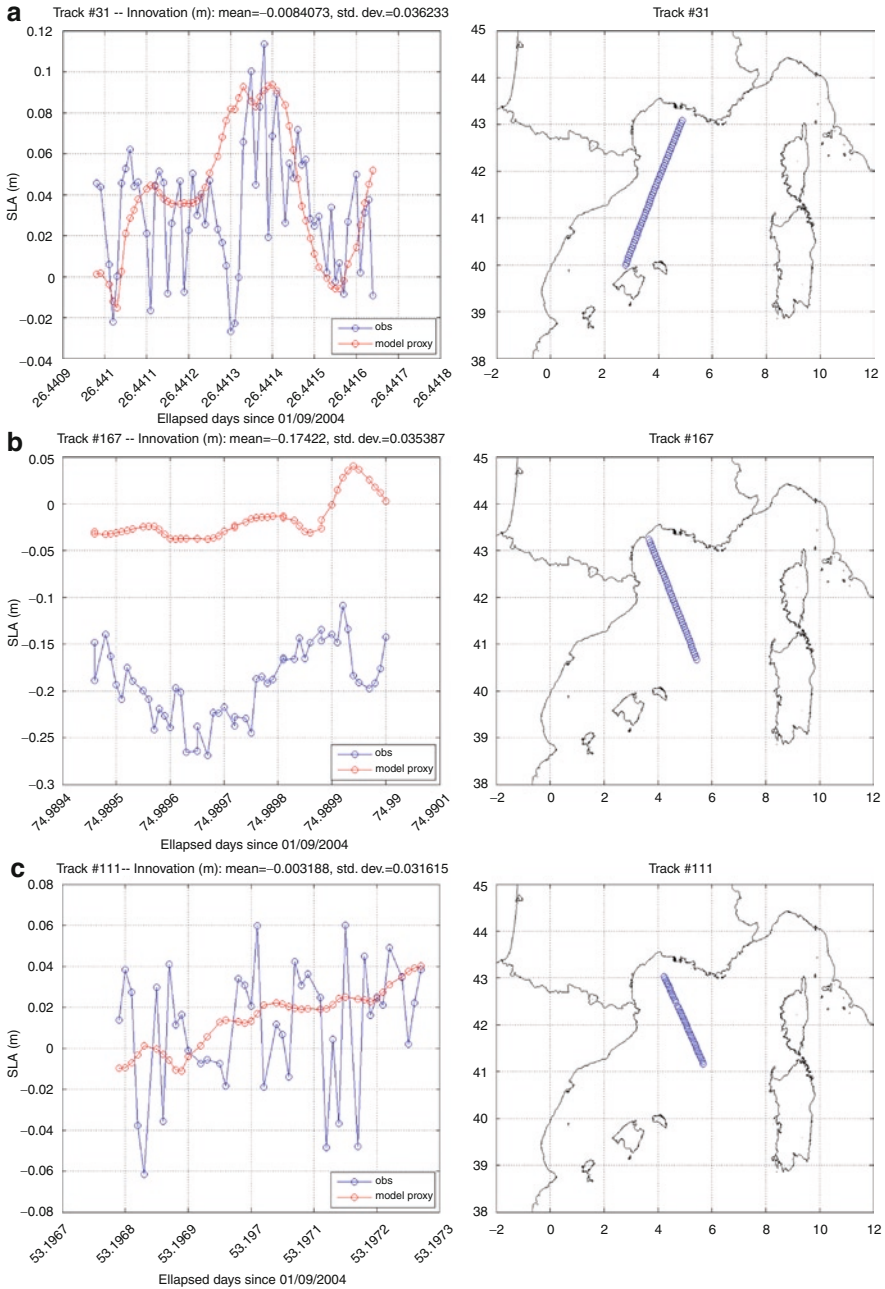


Fig. 9.7 Comparison between SYMPHONIE model sea surface elevation and X-TRACK corrected SLAs along (a) GFO track 031, (b) GFO track 401, (c) Jason-1 track 146, and (d) TOPEX/Poseidon track 009 in the NWMed Sea. Track locations are given on the associated right panels

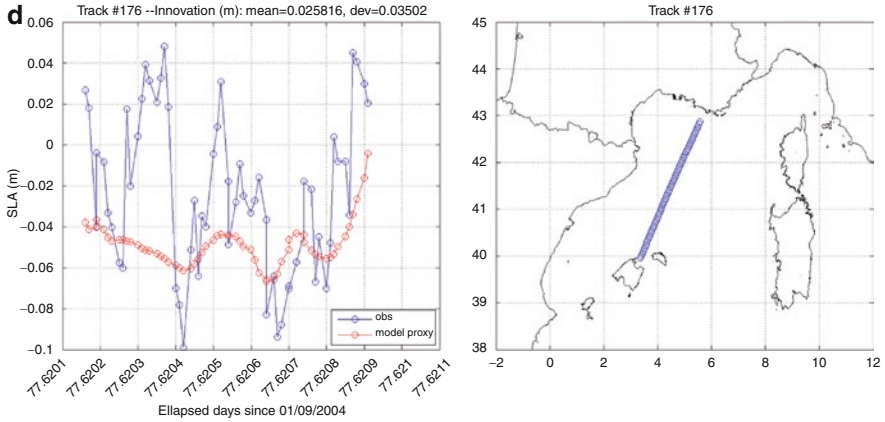


Fig. 9.7 (continued)

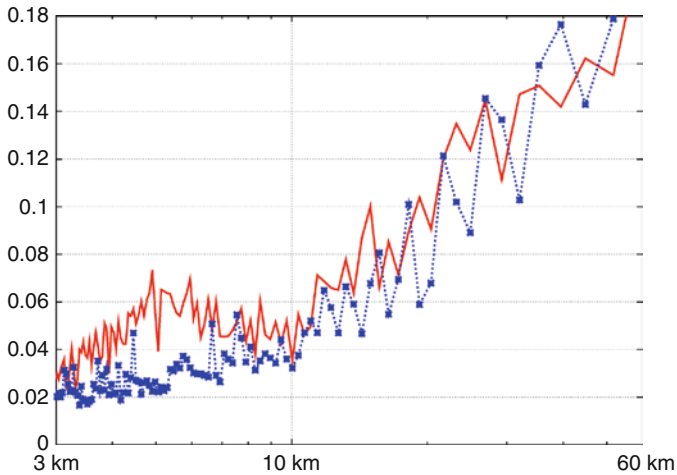


Fig. 9.8 Mean spatial power spectra: SYMPHONIE model sea surface elevation power spectrum (blue line) and T/P SLA estimates power spectrum (red line). Power amplitude is given in meters

9.4.3.2

Statistical Approach

Methodology

Another approach is to use a statistical analysis of the altimeter dataset itself to compute a steric correction. This consists in performing along-track singular value decomposition

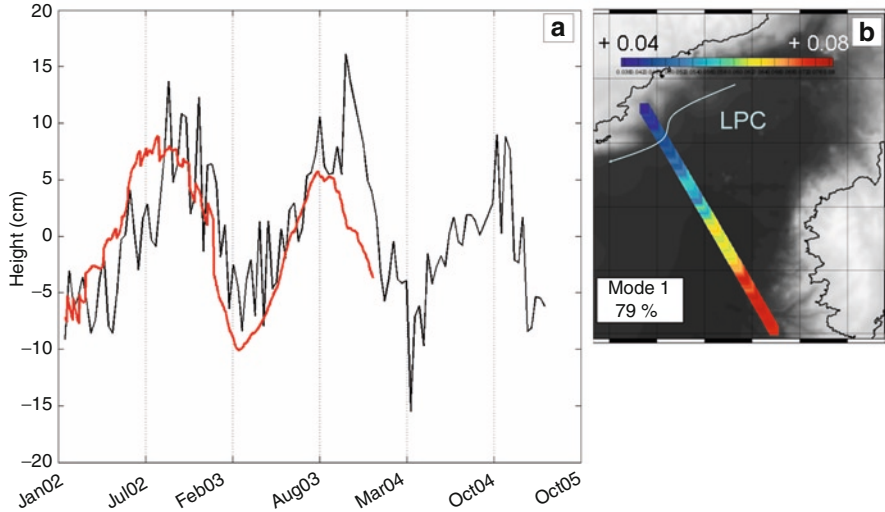


Fig. 9.9 Singular value decomposition of T/P SLAs along ground track 222. **(a)** First mode time component (rescaled by the singular value) and steric effect surface signature as computed from the SYMPHONIE model outputs. Unit is centimetres. **(b)** First mode spatial component (dimensionless)

(SVD) of the altimeter SLA time series. At seasonal time scales, sea surface variability is generally dominated by ocean currents and the annual large-scale steric signal. In this respect, in a statistics point of view, the first mode of the SVD would therefore represent this annual steric signal and could then be removed from the altimeter SLA. Unlike a high-pass digital filter with a cut-off period of 1 year, this method allows the altimetry to retain the variability of the annual dynamics (that is simulated in Boussinesq models) since the SVD method allows discrimination between coherent spatio-temporal dominant processes (from a statistical standpoint).

Case Study

This approach is illustrated through a case study over the Ligurian Sea. In this part of the NWMED Sea, the coastal section of the Jason-1 pass 222 intercepts the Liguro-Provençal-Catalan (LPC) Current quasi-perpendicularly (Fig. 9.9b). This coastal current flows seasonally and counter-clockwise along the continental slopes, from the Ligurian Sea to the Catalan Sea (e.g., Millot 1987, 1991). SLA estimates were computed with the X-TRACK processor for the Jason-1 pass 222 from January 2002 to December 2004.

Whereas modes greater than 1 represent less than 5% each, mode 1 is strongly dominant and represents 79% of the total energy. The associated time series (Fig. 9.9a, black curve) show a marked annual signal with negative and positive maxima respectively at the end of winter (March–April) and summer (September–October). The along-track structure of the mode 1 spatial component (Fig. 9.9b) shows a very small across-shore slope that would generate an insignificant across-track geostrophic flow. Compared to the strong across-track gradient featuring the LPC geostrophic zonal component, and noticing that the whole mode

1 spatial component is of same sign, this mode can be seen as a large-scale translation at the annual period. This suggests that this mode corresponds to the large-scale steric signals.

In order to validate this assumption, the time component has been compared with the steric time-dependent spatial constant built from the SYMPHONIE temperature and salinity fields following Eq. 9.9 (Fig. 9.9a, red curve). Fig. 9.9 shows that, although the modelled signal is smoother, the two signals agree very well in terms of magnitude and phasing which confirm that mode 1 represents the large-scale annual steric signal.

As a consequence, the mode 1 time evolution can be used for steric correction if the altimeter records are long enough (greater than 2 years) to be analysed using the SVD method. Unfortunately, this implies that this methodology is not applicable in operational conditions. Moreover, this methodology assumes that the annual steric effect surface signature is sufficiently marked over the area of interest to be isolated from the dynamic annual signal. This assumption would not be automatically verified in all shelf and coastal seas.

9.5

Concluding Remarks and Perspectives

The work initiated by the ALBICOCCA project and carried out at the CTOH/LEGOS in the NWMed has paved the way for improved post-processing of official altimeter products for coastal applications. Thanks to the X-TRACK processor, it is now possible to get more data close to the coasts (and even in open sea regions), with a reduced error budget (see also the chapter by Bouffard et al., this volume). In this coastal-oriented post-processing, in addition to more lenient editing criteria, land effects on the altimeter and radiometer measurements are minimized during the correction phase and missing or corrupted corrective terms are replaced by interpolation/extrapolation curves based on valid measurements. The X-TRACK processor benefits from state-of-the-art local modelling of tides and ocean response to wind and atmospheric pressure forcing as provided by the T-UGOm 2D (Mog2D follow-on) code for the de-aliasing of short-term barotropic signals and next generation models are expected to provide an even better accuracy. The high-resolution vertical reference frame needed to compute SLAs is locally adjusted using a consistent and coastal-tuned altimeter dataset.

However, features and processes of interest in the coastal systems are those which drive the local spatial variability on short time scales, constrained by the seabed and interaction with the mean flow, tides, seasonal cycles, inflow and outflow. In these conditions, additional developments are required within the X-TRACK processor in order to use several satellites (large-scale error reduction) with their higher acquisition rate leading to increased space and time sampling of altimeter observations.

Unquestionably, the X-TRACK processor will benefit in the future from advances in the new generation altimeters (Ka-band, Delay-Doppler, interferometry, etc.) and synergies with other sensors (tide gauges, SST, ocean colour, etc.). But the next major input in the short term should come from the pre-processing phase and improvements in wet tropospheric path delay correction. The retrieval of information from radar altimeter returned echoes and the decontamination of land effects in the radiometer measurements are

expected to be the source of a considerable reduction in the error budget of altimeter products in the future. Finally, major improvements are also expected from the update of regional tidal atlases.

This chapter also focused on matching coastal-oriented altimetry and regional circulation models. In the prospect of integrating altimeter data into models, the present study has pointed out the specific problem of taking into account the steric effect surface signature in regional ocean models that generally do not represent it well. Where possible, an SVD decomposition of altimeter SLA estimates would need to be performed in a delayed mode so that the steric and dynamic annual surface signatures could be statistically dissociable. In order to create physically consistent datasets, an alternate strategy, illustrated here for the NWMed, consists in removing from the altimeter SLA a steric height computed from a diagnostic equation and based on temperature and salinity fields computed by the model itself. However, such a strategy highly depends on the model used and forming and applying an operational correction term to altimetry observations computed from temperature and salinity (provided by forecasting systems for instance) remains a challenging issue.

This methodological work constitutes a first step toward assimilation of coastal altimetry into regional hydrodynamic models and opens up the way for an operational survey of coastal environments. However, numerous investigations still need to be made before the routine monitoring of coastal dynamics can become possible. First of all, small- and mesoscale dynamics are poorly or not reproduced in coastal models, except from a statistical point of view, whereas they seem to be captured in altimeter observations. Consequently, investigations need to be made in terms of hydrodynamic modelling in order to fully represent these scales. Comparisons with independent in situ measurements would also provide an idea of which scales are truly captured by satellite altimetry systems. The capabilities of data assimilation have been clearly demonstrated within the Global Ocean Data Assimilation Experiment (GODAE) for deep ocean or basin-scale systems and it now needs to be downscaled to regional level in coastal and shelf seas. This also requires substantial investigation in terms of data assimilation scheme definition and error settings, before running realistic experiments and finally real-time applications.

Acknowledgements The authors would like to thank the entire staff at the Centre de Topographie des Océans et de l'Hydrosphère (CTOH) at LEGOS for access to the altimeter data bases (<http://ctoh.legos.obs-mip.fr/>) and its expertise. This paper was significantly improved by comments from Rosemary Morrow. Very special thanks are due to Stefano Vignudelli and Paolo Cipollini for strong interactions on the coastal altimetry issue since the ALBICOCCA project. The ALBICOCCA project was funded by CNES in the framework of TOSCA programme and ASI. The SYMPHONIE model data come from the outcome of the MFSTEP project, funded by the European Commission 5th Framework Programme on Energy, Environment and Sustainable Development (EU contract number EVK3-CT-2002-00075). This work has been partially carried out in the framework of the "GOCE Gravity Improvement of Continental Slope and Shelf Ocean Circulation Modelling" study, funded by the European Space Agency (ESA contract number 19740/06/NL/HE). This work was carried out as a contribution to the MARINA (MARgin INtegrated Approach) project, funded by CNES in the framework of the Ocean Surface Topography Science Team investigation plan (CNES/EUMETSAT/NASA/NOAA).

In addition, the authors would like to honour the warmth and kind guidance of a pioneer, colleague and friend, Dr. Yves Ménard. This chapter is dedicated to his memory.

References

- Andersen OB (1999) Shallow water tides on the northwest European shelf from TOPEX/POSEIDON altimetry. *J Geophys Res* 104:7729–7741
- Andersen OB, Knudsen P (2000) The role of satellite altimetry in gravity field modelling in coastal areas. *Phys Chem Earth, Part A: Solid Earth Geodesy* 25(1): pp 17–24
- Antonov JI, Levitus S, Boyer TP (2002) Steric sea level variations during 1957–1994: importance of salinity. *J Geophys Res* 107(C12):8013
- Anzenhofer M, Shum CK, Rentsch M (1999) Coastal altimetry and applications, Tech. Rep. n. 464, Geodetic Science and Surveying, The Ohio State University, Columbus, USA
- Arakawa A, Suarez MJ (1983) Vertical differencing of the primitive equations in sigma coordinates. *Mon Wea Rev* 111:34–45
- Archiving, Validation, and Interpretation of Satellite Oceanographic Data (AVISO) (1996) In: Aviso Handbook for Merged TOPEX/Poseidon products, 3rd edn. Toulouse, France
- Berry PAM, Garlick JD, Freeman JA, Mathers EL (2005) Global inland water monitoring from multi-mission altimetry. *Geophys Res Lett* 32(16):1–4
- Birol F, Cancet M, Estournel C (2010) Aspects of the seasonal variability of the Northern Current (NW Mediterranean Sea) observed by altimetry. *J Mar Syst* 81(4):297–311
- Bouffard J, Roblou L, Ménard Y, Marsaleix P, De Mey P (2006) Observing the ocean variability in the western Mediterranean Sea by using coastal multi-satellite data and models. In: Proceedings of the Symposium on 15 years of Progress on Radar Altimetry, March 13–18, 2006, ESA SP-614, July 2006
- Bouffard J, Vignudelli S, Herrmann M, Lyard F, Marsaleix P, Ménard Y, Cipollini P (2008a) Comparison of ocean dynamics with a regional circulation model and improved altimetry in the Northwestern Mediterranean. *Terr Atmos Ocean Sci* 19:117–133
- Bouffard J, Vignudelli S, Cipollini P, Ménard Y (2008b) Exploiting the potential of an improved multimission altimetric data set over the coastal ocean. *Geophys Res Lett* 35:L10601
- Brown GS (1977) The average impulse response of a rough surface and its applications. *IEEE Trans Antennas Propag* 25:67–74
- Carrère L, Lyard F (2003) Modeling the barotropic response of the global ocean to atmospheric wind and pressure forcing – comparisons with observations. *Geophys Res Lett* 30(6):1275. doi:10.1029/2002GL016473
- Carton JA, Giese BS, Grodsky SA (2005) Sea level rise and the warming of the oceans in the Simple Ocean Data Assimilation (SODA) ocean reanalysis. *J Geophys Res* 110:C09006
- Chelton DB (2001) Report of the High-Resolution Ocean Topography Science Working Group Meeting, Oregon State
- Chelton DB, deSzoeke RA, Schlax MG, Naggar KE, Siwertz N (1998) Geographical variability of the first baroclinic Rossby Radius of deformation. *J Phys Oceanogr* 28:433–460
- Chelton DB, Ries JC, Haines BJ, Fu LL, Callahan PS (2001) Satellite altimetry. In: Fu L, Cazenave A (eds) *Satellite altimetry and earth sciences*, Int. Geophys. Ser., vol. 69. Elsevier, New York, pp 1–131
- Church JA, Godfrey JS, Jackett DR, Mc-Dougall TJ (1991) A model of sea level rise caused by ocean thermal expansion. *J Clim* 4:438–444
- Cipollini P, Gomez-Enri J, Gommenginger C, Martin-Puig C, Vignudelli S, Woodworth P, Benveniste J (2008a) Developing radar altimetry in the oceanic coastal zone: the COASTALT project. In: paper presented at General Assembly 2008, European Geoscience Union, Vienna, April 17–18
- Cipollini P, Vignudelli S, Lyard F, Roblou L (2008b) 15 years of altimetry at various scales over the Mediterranean. In: Vittorio Barale (JRC Ispra) and Martin Gade (Universitat Ambrugo) (eds) *Remote sensing of European Seas*. Springer, Heidelberg/Germany, pp 295–306

- Coppens D, Bijac S, Prunet P, Jeansou E (2007) Improvement of sea surface brightness temperature retrieval in coastal areas for the estimation of the wet tropospheric path delay. In: Paper presented at the Ocean Surface Topography Science Team meeting, Hobart, Australia
- Deng XL, Featherstone WE (2006) A coastal retracking system for satellite radar altimeter waveforms: application to ERS-2 around Australia. *J Geophys Res.* doi:10.1029/2005JC003039
- Desportes C, Obligis E, Eymard L (2007) On the wet tropospheric correction for altimetry in coastal regions. *IEEE Trans Geosci Remote Sensing* 45(7):2139–2149
- Dufau-Julliard C, Marsaleix P, Petrenko A, Dekeyser I (2004) Three-dimensional modelling of the Gulf of Lion's hydrodynamics (northwest Mediterranean) during January 1999 (MOOGLI3 Experiment) and late winter 1999: Western Mediterranean Intermediate Water's (WIW's) formation and its cascading over the shelf break. *J Geophys Res.* doi:10.1029/2003JC002019
- Durand F, Shankar D, Birol F, Shenoi SSC (2008) Estimating boundary currents from satellite altimetry: a case study for the east coast of India. *J Oceanogr* 64:831–845
- Estournel C, Kondrachoff V, Marsaleix P, Vehil R (1997) The plume of the Rhône: numerical simulation and remote sensing. *Cont Shelf Res* 17:899–924
- Estournel C, Durrieu de Madron X, Marsaleix P, Auclair F, Julliard C, Vehil R (2003) Observation and modelisation of the winter coastal oceanic circulation in the Gulf of Lions under wind conditions influenced by the continental orography (FETCH experiment). *J Geophys Res* 108(C3):1–18
- Estournel C, Auclair F, Lux M, Nguyen C, Marsaleix P (2007) "Scale Oriented" embedded modelling of the North-Western Mediterranean in the frame of MFSTEP. *Ocean Sci Discuss* 4:145–187
- Fernandes MJ, Bastos L, Antunes M (2003) Coastal satellite altimetry – methods for data recovery and validation. In: Tziavo IN (ed) Proceedings of the 3rd meeting of the International Gravity & Geoid Commission (GG2002), Editions ZITI, pp 302–307
- Fu LL, Cazenave A (2001) Satellite altimetry and earth sciences: a handbook of techniques and applications. *Int Geophys Ser*, vol 69. Elsevier, New York
- Gaspar P, Ponte RM (1997) Relation between sea level and barometric pressure determined from altimeter data and model simulations. *J Geophys Res* 102(C1):961–971
- Gatti J, Petrenko A, Devenon JL, Leredde Y, Ulses C (2006) The Rhone river dilution zone present in the northeastern shelf of the Gulf of Lion in December 2003. *Cont Shelf Res* 26:1794–1805
- Gregory JM (1993) Sea level changes under increasing atmospheric CO₂ in a transient coupled ocean-atmosphere GCM experiment. *J Clim* 6(12):2247–2262
- Greatbatch RJ (1994) A note on the representation of steric sea levels in models that conserve volume rather than mass. *J Geophys Res* 99(12):767–771
- Guizien K, Brochier T, Duchène JC, Koh BS, Marsaleix P (2006) Dispersal of *owenia fusiformis* larvae by wind-driven currents: turbulence, swimming behaviour and mortality in a three-dimensional stochastic model. *Mar Ecol Prog Ser* 311:47–66
- Han G, Tang CL, Smith PC (2002) Annual variations of sea surface elevation and currents over the Scotian Shelf and Slope. *J Phys Ocean* 32:1794–1819
- Herrmann M, Somot S, Sevault F, Estournel C, Déqué M (2008) Modelling the deep convection in the northwestern Mediterranean Sea using an eddy-permitting and an eddy-resolving model: case study of winter 1986–1987. *J Geophys Res.* doi:10.1029/2006JC003991
- Hernandez F, Calvez MH, Dorandeu J, Faugère Y, Mertz F, Schaeffer P (2000) Surface Moyenne Océanique: Support scientifique à la mission altimétrique Jason-1, et à une mission micro-satellite altimétrique. Contrat Ssalto 2945 – Lot 2 – A.1. Rapport d'avancement. Rapport n° CLS/DOS/NT/00.313, published by CLS, Ramonville St Agne, pp 40
- Hirose N, Fukumori I, Zlotnicki V (2001) Modelling the high frequency barotropic response of the ocean to atmospheric disturbances: sensitivity to forcing, topography and friction. *J Geophys Res* 106(C12):30987–30995
- Ishii M, Kimoto M, Sakamoto K, Iwasaki SI (2006) Steric sea level changes estimated from historical ocean subsurface temperature and salinity analyses. *J Oceanogr* 62(2):155–170

- Jan G, Ménard Y, Faillot M, Lyard F, Jeansou E, Bonnefond P (2004) Offshore absolute calibration of space borne radar altimeters. *Mar Geod. Special issue on Jason-1 calibration/validation, Part 3*, 27:3–4, 615–629
- Jorda G, Comerma E, Bolaños R, Espino M (2007) Impact of forcing errors in the CAMCAT oil spill forecasting system. A sensitivity study. *J Mar Syst* 65:134–157
- Köhl A, Stammer D (2008) Variability of the meridional overturning in the North Atlantic from the 50-year GECCO state estimation. *J Phys Oceanogr* 38:1913–1930
- Labroue S, Gaspar P, Dorandeu J, Zanifé OZ, Mertz F, Vincent P, Choquet P (2004) Non parametric of the sea states bias for Jason 1 radar altimeter. *Mar Geod* 27:453–481
- Lambin J, Lombard A, Picot N (2008) CNES initiative for altimeter processing in coastal zone: PISTACH. In: Paper presented at the First altimeter workshop, Silver Spring, MD, February 5–7
- Le Hénaff M, Roblou L, Bouffard J (2010) Characterizing the Navidad Current interannual variability using coastal altimetry. *Ocean Dyn* (in press)
- Le Provost C (2001) Ocean tides. In: Fu LL, Cazenave A (eds) *Satellite altimetry and earth sciences: a handbook of techniques and applications*. *Int Geophys Ser*, vol 69. Academic, San Diego, CA, pp 267–303
- Le Traon PY, Ogor F (1998) ERS-1/2 orbit improvement using TOPEX/POSEIDON: the 2cm challenge. *J Geophys Res* 103:8045–8057
- Lombard A, Cazenave A, Le Traon PY, Guinehut S, Cabanes C (2006) Perspectives on present day sea level change: a tribute to Christian Le Provost. *Ocean Dyn* 56:445–451
- Lombard A, Garric G, Penduff T (2009) Regional patterns of observed sea level change: insights from a ¼° global ocean/sea-ice hindcast. *Ocean Dyn*. doi:10.1007/s10236-008-0161-6
- Lyard F, Lefevre F, Letellier T, Francis O (2006) Modelling the global ocean tides: modern insights from FES2004. *Ocean Dyn*. doi:10.1007/s10236-006-0086-x
- Lyard F, Roblou L, Mangiarotti S, Marsaleix P (2003) En route to coastal oceanography from altimetric data: some ALBICOCCA project insight. In: Paper presented at the Ocean surface topography science team meeting, Arles, France
- Lyard F, Roblou L (2009) Robust methods for high accuracy tidal modelling in coastal and shelf seas. In: Paper presented at the Ocean Surface Topography Science Team meeting, Seattle, Washington, DC, USA
- Lyard F, Roblou L, De Mey P, Lamouroux J (2009) Ocean high frequency dynamics at global and regional scales. In: Paper presented at the first SARAL/AltiKa scientific workshop, Ahmedabad, India
- Lynch DR, Gray WG (1979) A wave equation model for finite element tidal computations. *Comput Fluids* 7:207–228
- Mangiarotti S, Lyard F (2008) Surface pressure and wind stress effects on sea level change estimations from TOPEX/Poseidon satellite altimetry in the Mediterranean Sea. *J Atmos Ocean Technol* 25:464–474
- Mantripp D (1996) Radar altimetry. In: Fancey NE, Gardiner ID, Vaughan RA (eds) *The determination of geophysical parameters from space*. Scottish Universities Summer School in Physics and Institute of Physics Publishing, Bristol/Philadelphia
- Manzella GMR, Borzelli GL, Cipollini P, Guymer TH, Snaith HM, Vignudelli S (1997) Potential use of satellite data to infer the circulation dynamics in a marginal area of the Mediterranean Sea. In: *Proceedings of 3rd ERS symposium – space at the service of our environment*, Florence (Italy), 17–21 March 1997, vol 3, pp 1461–1466, European Space Agency Special Publication ESA SP-414
- Maraldi C, Galton-Fenzi B, Lyard F, Testut L, Coleman R (2007) Barotropic tides of the Southern Indian Ocean and the Amery Ice Shelf cavity. *Geophys Res Lett*. doi:10.1029/2007GL030900
- Marsaleix P, Auclair F, Estournel C (2006) Considerations on open boundary conditions for regional and coastal ocean models. *J Atmos Ocean Technol* 23:1604–1613
- Marsaleix P, Auclair F, Floor JW, Herrmann MJ, Estournel C, Pairaud I, Ulses C (2008) Energy conservation issues in sigma-coordinate free-surface ocean models. *Ocean Model* 20:61–89

- Millot C (1987) Mesoscale and seasonal variabilities of circulation in western Mediterranean. *Dyn Atmos Ocean* 15:179–214
- Millot C (1991) Circulation in the western Mediterranean. *Oceanol Acta* 10:143–149
- Morrow R, Valladeau G, Sallee JB (2008) Observed subsurface signature of Southern Ocean sea level rise. *Prog Oceanogr* 77(4):351–366. A new view of water masses after WOCE. A special edition for Professor Matthias Tomczak
- Ollivier A, Le Bihan N, Lacoume JL, Zanife OZ (2005) Improving speckle filtering with SVD to extract ocean parameters from altimetry radar echos. In: *Proceeding of PSIP 2005*, Toulouse
- Pairaud I, Lyard L, Auclair F, Letellier T, Marsaleix P (2008) Dynamics of the semi-diurnal and quarter-diurnal internal tides in the Bay of Biscay. Part 1: barotropic tides. *Cont Shelf Res*. doi:10.1016/j.csr.2008.03.004
- Pascual A, Faugère Y, Larnicol G, Le Traon PY (2006) Improved description of the mesoscale variability by combining four satellite altimeters. *J Geophys Res*. doi:10.1029/2005GL024633
- Pattullo J, Munk W, Revelle R, Strong E (1955) The seasonal oscillation in sea level. *J Mar Res* 14:88–156
- Petrenko A, Leredde Y, Marsaleix P (2005) Circulation in a stratified and wind-forced Gulf of Lions, NW Mediterranean Sea: in-situ and modelling data. *Cont Shelf Res* 25:7–27
- Quesney A, Jeansou E, Lambin J, Picot N (2007) A new altimeter waveform retracking algorithm based on neural networks. In: *Paper presented at the Ocean surface topography science team meeting*, Hobart, Australia
- Roblou L (2004) Validation des solutions de marée en Mer Méditerranée: comparaisons aux observations. Technical Report, POC-TR-02-04, 67pp, Pôle d’Océanographie Côtière, Toulouse, France
- Roblou L, Lyard F, Le Hénaff M, Maraldi C (2007) X-TRACK, a new processing tool for altimetry in coastal ocean. In: *ESA ENVISAT Symposium*, Montreux, Switzerland, April 23–27, 2007, ESA SP-636, July 2007
- Ruf CS, Keihm SJ, Subramanya B, Janssen MA (1994) TOPEX/Poseidon microwave radiometer performance and in-flight calibration. *J Geophys Res* 99(C12):24915–24926
- Service d’Altimétrie et de Localisation Précise (SALP) (1996) Minutes of the ocean surface topography science team meeting, Venice, Italy, March 16–18, 2006, SALP-CR-MA-EA-15640-CNES, Y. Ménard (ed), CNES, p 90
- Stammer D, Wunsch C, Ponte RM (2000) De-aliasing of global high frequency barotropic motions in altimeter observations. *Geophys Res Lett* 27(8):1175–1178
- Tai CK (1989) Accuracy assessment of widely used orbit error approximations in satellite altimetry. *J Atmos Ocean Technol* 6:147–150
- Tai CK (1991) How to observe the gyre to global-scale variability in satellite altimetry: signal attenuation by orbit error removal. *J Atmos Ocean Technol* 8:271–288
- Tournadre J (2006) Improved level-3 oceanic rainfall retrieval from dual-frequency spaceborne radar altimeter systems. *J Atmos Ocean Technol*. doi:10.1175/JTECH1897.1
- Tomczak M, Godfrey JS (1994) *Regional oceanography: an introduction*. Pergamon, New York
- Ulses C, Grenz C, Marsaleix P, Schaaff E, Estournel C, Meulés S, Pinazo C (2005) Circulation in a semi enclosed bay under the influence of strong fresh water input. *J Mar Syst* 56:113–132
- UNESCO, ICES, SCOR, IAPSO (1981) Background papers and supporting data on the international equation of state of seawater, 1980, UNESCO technical papers in Mar Science. Nr. 38, UNESCO
- Vignudelli S, Cipollini P, Astraldi M, Gasparini GP, Manzella GMR (2000) Integrated use of altimeter and in situ data for understanding the water exchanges between the Tyrrhenian and Ligurian Seas. *J Geophys Res* 105(19):649–663
- Vignudelli S, Cipollini P, Roblou L, Lyard F, Gasparini GP, Manzella G, Astraldi M (2005) Improved satellite altimetry in coastal systems: case study of the Corsica Channel (Mediterranean Sea). *Geophys Res Lett*. doi:10.1029/2005GL022602
- Volkov DL, Larnicol G, Dorandeu J (2007) Improving the quality of satellite altimetry data over continental shelves. *J Geophys Res*. doi:10.1029/2006JC003765
- Wunsch C, Ponte R, Heimbach P (2007) Decadal trends in sea level patterns: 1993–2004. *J Clim* 20:5889–5911